inter.noise
21-24 AUGUST
SCOTTISH EVENT CAMPUS
GLASGOW 2022

Numerical investigation of power flow input into a fuselage due to jet engine induced wing vibrations

Sebastian F. Zettel[1] | René Winter[2] | Marco Norambuena[3] | Thomas Klimmek[4] | Marc Böswald[5]

German Aerospace Center (DLR), Institute of Aeroelasticity, Bunsenstraße 10, 37073 Göttingen

ABSTRACT

The wings of passenger aircrafts are constantly vibrating due to various loads. There are low-frequency vibrations caused by transient gust loads and broad band stationary vibration caused by natural turbulence. In addition, there are also higher-frequency multi-harmonic vibrations caused by the vibration loads of the jet engines. The kinetic energy of the higher-frequency stationary vibrations of the wing are partially transferred as a power flow into the fuselage, where some part of this vibration energy may be radiated as sound, which is then perceived as noise by the passengers and the crew. This work is part of the EU CleanSky2 framework. The chain of energy transfer effects in an airframe is being investigated in more detail aiming for the quantification of the vibrational power flow input into the fuselage by utilizing structural intensity. Numerical investigations are carried out on FEM models of an Airbus A320 wing generated with a parametric model generator. Focus will be the quantification of power flow input into the fuselage in dependence of the engine installation point on the wing. This is achieved by varying the excitation locations along the wing and also the excitation directions. In the further course of the project, these numerical results will be validated by a test campaign. For this purpose, a real wing of an A320 is available as a test structure.

1. INTRODUCTION

The wing is the main transfer path for engine induced vibrations entering the fuselage. The vibrational power input flows from the engine through the pylon into the wing and eventually into the fuselage structure, see Figure 1. The vibrating fuselage structure emits sound into the cabin cavity and thus onto the passengers. So far there are no detailed investigations on the quantification of the power flow magnitude injected into the fuselage by the engine induced vibrations. Accordingly, the opportunities to use the wing with its transfer paths as a means for cabin noise reduction has also not been studied extensively.

[1] Sebastian.Zettel@dlr.de

[2] Rene.Winter@dlr.de

[3] Marco.Norambuena@dlr.de

[4] Thomas.Klimmek@dlr.de

[5] Marc.Boeswald@dlr.de

In the EU CleanSky2 framework an experimental test campaign on a full scale A320 wing is planned. The goals are to update a respective A320 wing Finite Element Method (FEM) model for numerical estimations of the power flow and to experimentally estimate the power flow in the wing. In both cases utilizing the structural intensity (STI) as an indicator for the power flow. The power flow levels will be estimated for varying excitation locations to gain insight on how the power input into the fuselage varies for engine positions along the wing. This is especially interesting in terms of current developments towards distributed propulsion systems on future wing structures as well as future designs with larger engines installed close to the fuselage.

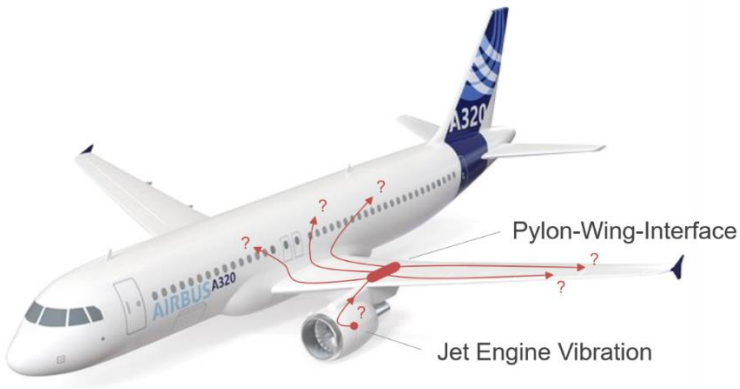

Figure 1: Visualization of vibrational power flow transfer paths [1]

In Chapter 2 the setup of the planned experiment will be described. This will also cover the approach of exciting the wing structure with a multiaxial shaker setup to imitate engine vibration in operation. Furthermore, the FE model representing the A320 wing for the numerical study will be presented and the theoretical foundation to calculate STI values from FEM results will be stated for shell and beam elements.

Chapter 3 presents the numerical study, the respective results for power flow levels entering the fuselage depending on varying excitation locations along the wing.

2. METHODS AND PLANNED EXPERIMENTS

This chapter presents the general setup of the planned experiment in subchapter 2.1, the fundamentals of the structural intensity in subchapter 2.2 and how the current numerical investigation is conducted in subchapter 2.3.

2.1. Experimental Setup

The experimental setup will provide a mounting of the wing in a way that real-world interfaces are being used to install the wing on a test rig. Meaning, the wing will be mounted in a support imitating the fuselage connection, see Figure 2. As the manufacturing of the wing support structure was not completed while this manuscript has been compiled, a detailed construction cannot be provided here.

The wing structure will be excited with a multiaxial shaker setup that has also been developed in the ADEC Project within the EU CleanSky LPA framework [2]. It has been designed for the control of multiple shakers with the aim of reproduction of combined multi-point dynamic force and torque excitation. This allows to imitate vibrations of jet engines under stationary flight conditions along and about several axes at once. The target vibration signals will be estimated by a jet engine vibration

source model currently under development in the DLR project INTONATE (Future Aircraft Interior Noise and Vibration Evaluation).

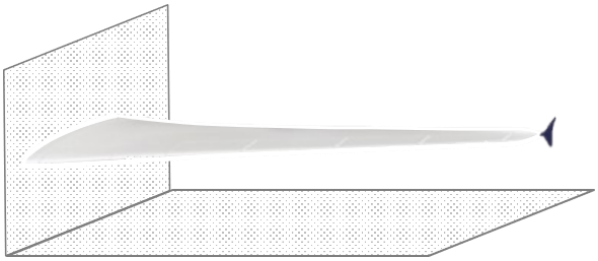

Figure 2: Wing structure mounting for experiment [1]

The resulting vibrations of the excited wing will be measured using methods available for high density vibrational measurements like scanning Laser-Doppler-Vibrometers or rowing grid sensors. The acquired measurement data will then be assessed with in-house developed software which allows to estimate the STI for complex lightweight structures such as wing and fuselage structures.

2.2. Structural Intensity based on FEM results

Structural Intensity (STI) is a vector quantity describing the vibrational power flow per unit area through a structure. The STI is calculated by utilizing nodal velocities (translations and rotations) with the stresses acting in the elements. By multiplying the STI or the element stresses with the cross-sectional area in flow direction it is possible to acquire the power flow in the unit Watt directly. The power flow for plate elements in x- and y-direction (in-plane directions) while neglecting the z-direction (out of plane direction) can be described by

$$P_{x,s} = -\frac{1}{2} \cdot Re\left\{N_{x,s} \cdot {v_x}^* + N_{xy,s} \cdot {v_y}^* + M_{x,s} \cdot {\omega_y}^* + M_{xy,s} \cdot {\omega_x}^* + Q_{xz,s} \cdot {v_z}^*\right\}$$

$$P_{y,s} = -\frac{1}{2} \cdot Re\left\{N_{y,s} \cdot {v_y}^* + N_{xy,s} \cdot {v_x}^* + M_{y,s} \cdot {\omega_x}^* + M_{xy,s} \cdot {\omega_y}^* + Q_{yz,s} \cdot {v_z}^*\right\}$$

with N_i – normal element forces, M_i – element bending moments, Q_i – element shear forces in out-of-plane direction, ${v_i}^*$ – complex conjugated nodal velocities, ω_i – complex conjugated nodal rotation speeds and the sub-index s indicating the values for shell elements [3]. All values and also the resulting intensities are time averaged and frequency dependent values. Peak quantities are used.

On the other hand, the power flow for beam elements can be described by

$$P_b = -\frac{1}{2} \cdot Re\left\{N_{x,b} \cdot {v_x}^* + T_b \cdot {\omega_x}^* - M_{y,b} \cdot {\omega_y}^* + M_{z,s} \cdot {\omega_z}^* + Q_{xz,b} \cdot {v_z}^* + Q_{xy,b} \cdot {v_y}^*\right\}$$

with T_i – torsion along beam and the sub-index b indicating the values for beam elements [3].

2.3. Numerical representation of A320 wing adapted for power flow estimation

The initial FE model of the wing is created by a parametric model generator (DLR software ModGen) which is focused on either creating simplified dynamic models for aircraft preliminary design but also detailed models as required for load analysis [4] or respectively for sizing of aircraft components. The model, the right wing (when looking in flight direction), consists of the full wing modelled as a box-beam containing ribs, stringers, spars as well as upper and lower wing skins, see Figure 3. Most of the model consists of shell elements while the stringers are modelled with beam elements. These

beam elements cannot be distinguished easily in the graphical display of the model, because they are plotted as lines which coincide with edges of the shell elements. The model contains one half of the center wing box (CWB) which connects the wing structure to the main aircraft structure in the bottom part of the fuselage. The model currently misses a detailed pylon structure. Thus, the forces introduced from the engine into the wing over the pylon will be applied directly to the wing structure.

The goal was to setup an initial FE model allowing the assessment of the power flow entering the fuselage structure. The chain of effects for this is as follows. An excitation of the wing generates vibrational waves traveling throughout it. These eventually enter the CWB. Before entering the CWB, waves are partially reflected at the interface between main wing structure and CWB due to the enveloping fuselage structure and its stiffness. As the center wing box is a part of the fuselage structure and has various connection points to it, the wave energy entering the center wing box flows into the fuselage structure and is dissipated by the elastic deformation of the airframe and its structural damping. Partially, the wave energy also flows into the surrounding fluid (i.e. the aerodynamic damping of the surrounding flow-field) but more critically, the wave energy can also flow into the cabin cavity.

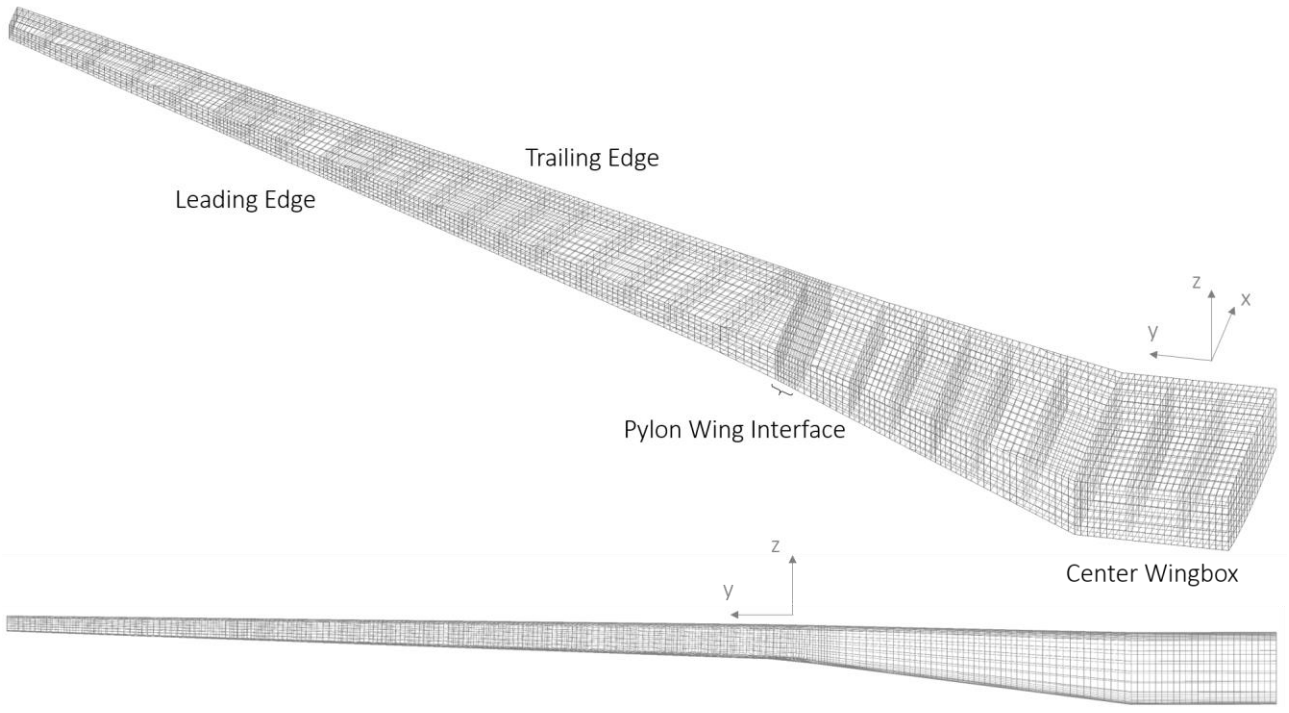

Figure 3: A320 wing box FE model, upper: iso view, lower: frontal view on leading edge

The model was setup to imitate this behavior. The nodes of the free end of the CWB are fully constrained to model a fixed support, see red indicator Figure 4a.

The nodes, which form the outer shape of the model, along the interface between main wing structure and CWB, see green indicator in Figure 4a, are all assigned with spring elements representing the stiffness of the enveloping fuselage structure. Even though there is currently no fuselage model available, the stiffness was estimated by calculating the stiffness of the CWB for bending about the x- and z-axis for forces acting at the interface between main wing structure and CWB. The resulting stiffness was then distributed to the outer nodes along the interface to model an approximate stiffness of the fuselage.

In general, the fuselage is a sink for vibrational energy of the wing. Since the fuselage is not part of the model, this effect of energy sink has to be modelled in a substitute way. To simulate the outflow of wave energy from the CWB into the fuselage structure the nodes located three rows ahead of the fully constrained nodes of the boundary condition, see Figure 4b, are assigned with dash pot dampers. Like this, the wave energy entering the CWB flows through it but a big amount is dissipated in the dash pot dampers. This also adds a known local energy sink into the system. This adds certainty to the direction of the power flow inside the CWB as wave energy tends to flow towards regions of high dissipation [5]. Only one line of dash pot dampers is assigned to influence the structural system as least as possible regarding its response.

Except for the ring of dashpot dampers, the energy dissipation throughout the wing structure is modelled with distributed structural damping (i.e. stiffness proportional structural damping). Due to the complexity of the wing box as well as CWB structure and the fact that many parts are joined by rivets [6] the structural damping is set to $\eta = 0.04$ which is much higher than the $\eta = 0.005$ usually applied for simple monolithic aluminum structures. However, this structural damping is just an initial estimation and measurement data will show if it is a valid assumption.

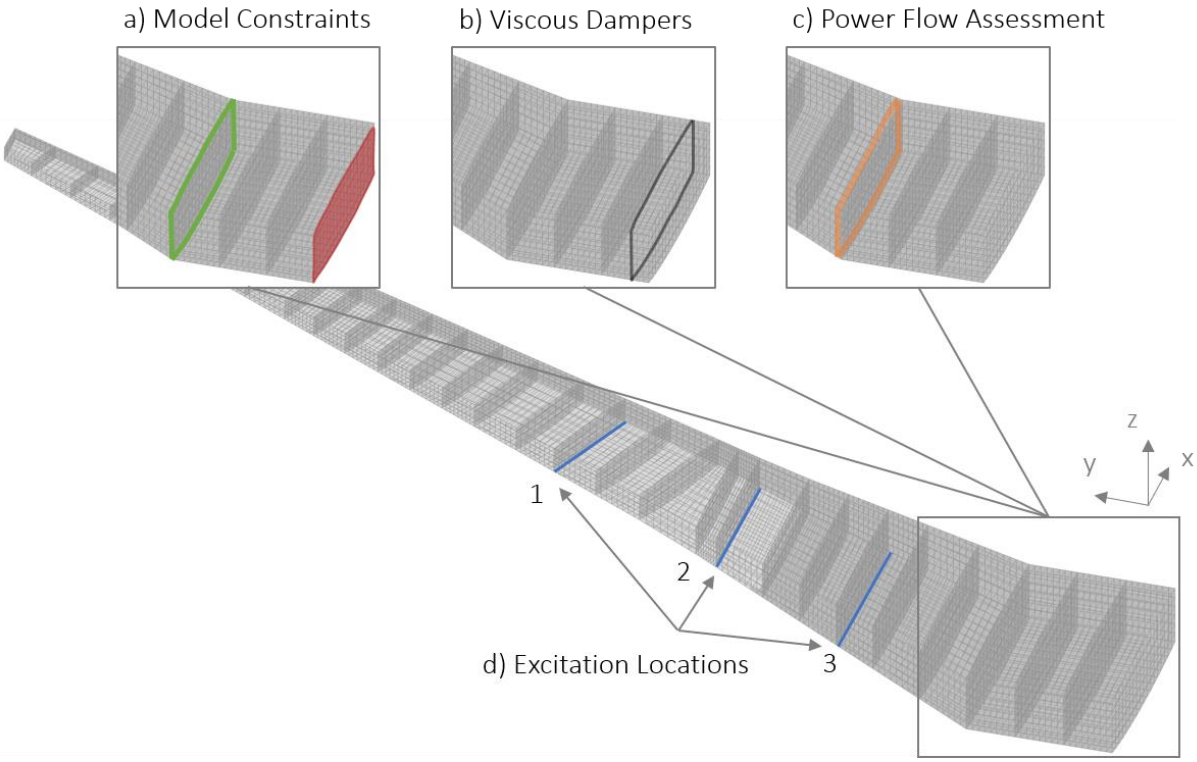

Figure 4: Wing FE model with zooms, a) model constraints – green: spring elements, red: fixed boundary condition b) viscous damper location, c) power flow assessment location, d) excitation locations

The excitation of the wing is realized at three distinct locations along the wing, see Figure 4d. Excitation location “2” is the original pylon position where the engine is attached. Excitation location “1” is more outboard and “3” is located more inboard in relation to the original engine attachment point. These positions are chosen in order to show to what extend the resulting power flow in the CWB scales with possible varying engine positions along the wing.

For every excitation location, in-phase forces are applied along the nodes in chord-wise direction at the lower wing surface however only on nodes which coincide with ribs. This line force approach was chosen to counter current unknown model behavior due to point loads. The summation of forces for every excitation location are equal and have a constant amplitude of 1N over the investigated frequency range.

The model is not yet optimized for a comparison of excitation locations as only the part of the wing where the engine is usually fitted has a proper stiffening with additional ribs to carry the engine loads. The stiffened pylon attachment of the current wing layout might act as barrier towards the CWB for vibrational waves arriving from excitation “1” and act as reflector towards the CWB for vibrational waves arriving from excitation “3”. A necessity for a representative comparison for these three excitation locations are distinct wing layouts with specifically modelled stiffeners for the respective locations. However, the currently used FE model will show if the chosen approach results in physically meaningful results.

During operation, jet engines generate vibrations due to unbalance forces in the directions perpendicular (y- and z- direction) to the rotation axis of the engine shaft. Additionally, the engines experience vibrations along the x-direction induced by fluctuations of thrust based on disturbances of the air flow of the engine-intake. This is the reason the FE model will be separately excited in x-, y- and z-direction to show the influence of the single vibration direction on the power flow in the CWB.

The resulting power flow in the CWB which is assumed to be the power flow entering the fuselage is assessed over the line of elements shown in Figure 4c. Not only the power flow through the shell elements but also through the beam elements will be considered.

A frequency range of 20 Hz to 450 Hz will be considered in this study. The lower frequency limit is set to 20 Hz because this marks the general lower limit for hearable frequencies. The upper frequency limit is set to 450 Hz (upper frequency limit of the 1/3 octave band with 398 Hz center frequency) based on findings from a preceding study. The mentioned study performed a wavenumber analysis on structural response data acquired during a measurement campaign of the Acoustic Flight Laboratory structure at the Center for Applied Aeronautics Research in Hamburg, Germany [7]. The results showed that the mid-frequency range of the investigated fuselage extends from about 150 Hz up to 300 Hz. A strong interaction between structural vibrations and acoustics are present in the mid-frequency range and thus the wing vibrations in this frequency range are important to be assessed. From 300 Hz upwards the high-frequency range begins, which is dominated by statistical structural behavior and needs different tools, like the Statistical Energy Analysis [8] or the Dynamical Energy Analysis [9], to be properly assessed. As these frequency boundaries between the frequency domains are likely to vary for different aircraft fuselages the upper frequency limit is increased by 50% to take this fact into consideration.

3. NUMERICAL STUDY

This chapter presents the results of the power flow assessed in the CWB at the location shown in Figure 4b. Figure 5 presents an example of the calculated STI fields at 230 Hz. Originating from the excitation (red indication) the wave energy flows towards both ends of the wing. The wing is a box assembly and the wave energy thus can flow between front and rear spar as well as the upper and lower skin surfaces by using the ribs as transfer paths. At 230 Hz the upper and lower skins of the wing mainly introduce power into the CWB. In the CWB, at the region located close to the line of dash pot dampers the power flow vectors decrease rapidly because of the high dissipation effect.

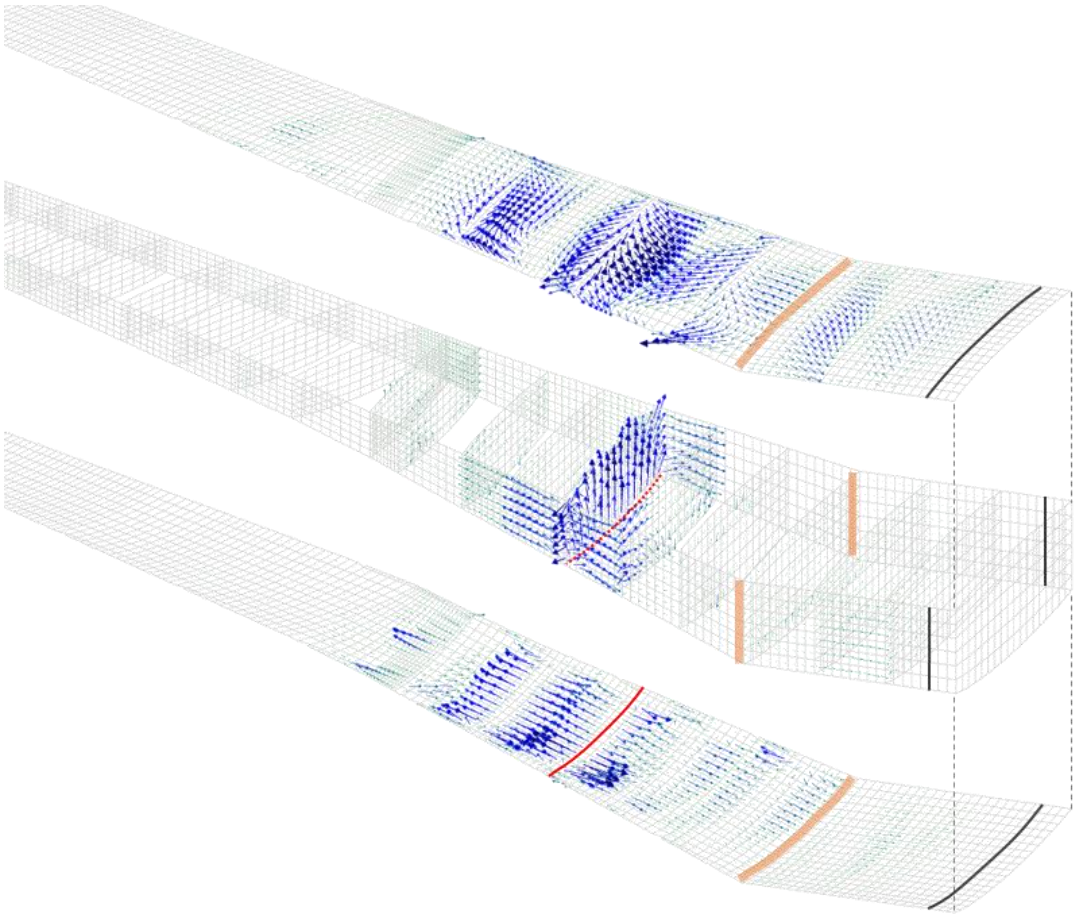

Figure 5: Structural intensity plot at 230 Hz for excitation at location "2" in z-direction with normalized power flow vectors, red: excitation location, orange: power flow assessment location, black: dash pot damper location

The assessment of the power flows entering the CWB are presented in bar charts utilizing 1/3 octave bands. Positive values indicate power flows entering the CWB and negative values leaving the CWB. For every frequency step, the discrete power flow values of each individual element along the assessment line, see Figure 4b, the sum is formed. Subsequently, for every considered frequency band the according previously calculated power flow sums are added up, which finally form the total values used in the following bar plots.

Figure 6 presents the results for the power flow assessment of the model for excitations in z-direction. In the lower frequency region up 100 Hz, power flows are almost not existent. In some cases, they are even negative which indicates an outflow of wave energy from the CWB. Starting with the 100 Hz band the power flows entering the CWB start to rise. A clear trend of higher power flows for excitations located closer to the fuselage can be seen except for bands at 100 Hz and 158.5 Hz. A possible, but as of now not investigated, reason for this behavior might be resonance effects in this frequency range. In some frequency ranges the chosen excitation locations might be beneficial for inducing the structure but in other frequency ranges the same locations might be unfavorable. The negative power flows are assumed to be connected to the large displacements of the main wing structure at low frequencies and the resulting high strain areas which cause dissipation.

The results for power flows entering the CWB for excitation in x-direction, see Figure 7, show a similar trend. At lower frequencies up to 100 Hz the power flows are again almost zero and thus are neglected here. Furthermore, the power flows are again rising for higher frequencies.

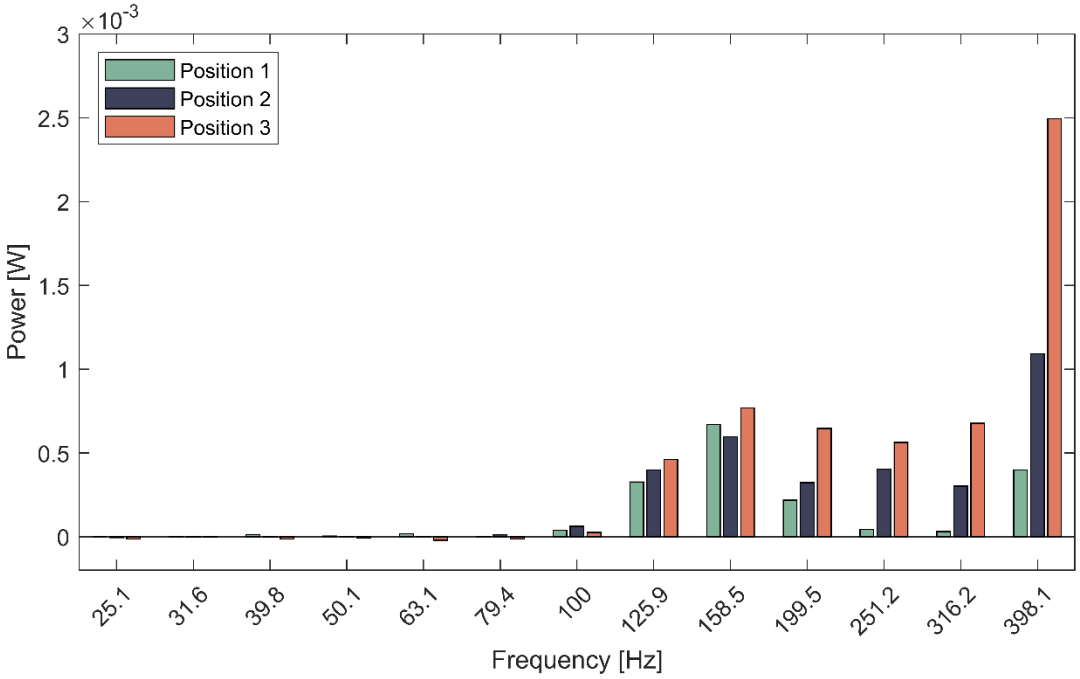

Figure 6: Power flow assessment for excitations in z-direction

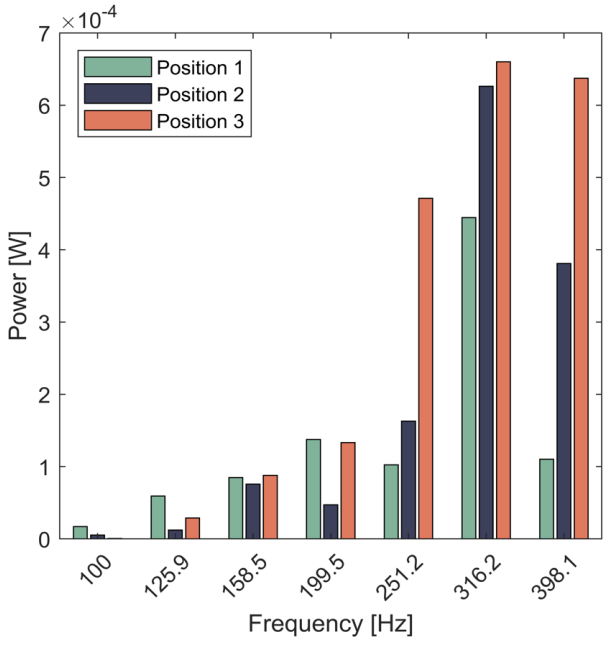

Figure 7: Power flow assessment for excitations in x-direction

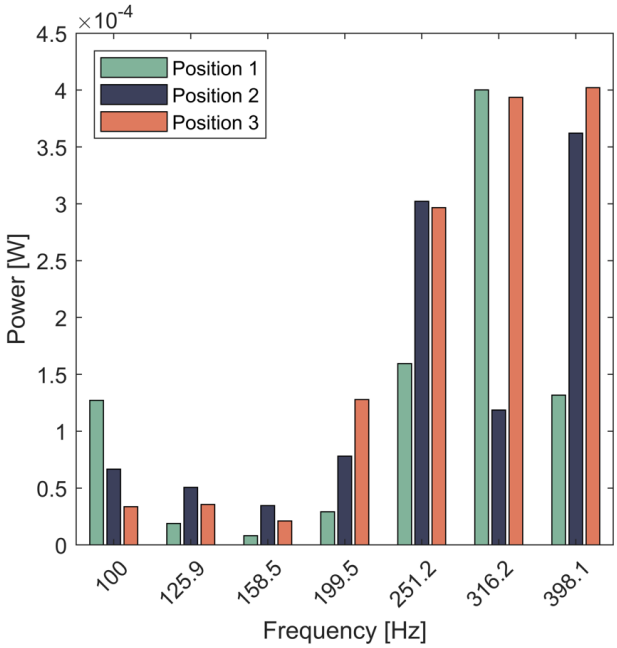

Figure 8: Power flow assessment for excitations in y-direction

However, the power flows are on average only 30% as high as for the excitation in z-direction. The reason is the higher structural stiffness of the wing in x-direction. With less flexibility, the same excitation force can simply not perform the same amount of mechanical work. For excitations in x-direction there is no clear trend of higher power flows for excitations closer to the fuselage in frequency bands as low as for excitations in z-direction. Only starting from 251.2 Hz there is a clear trend. Below that frequency band the power flows for varying excitation locations do not show a clear and consistent trend.

Figure 8 presents the power flow results for excitations in y-direction. Just like before the power flows up to the 100 Hz band are almost zero and are neglected. Up to the 199.5 Hz band the magnitudes of power flows are about as high as for the excitation in x-direction. However, the peak values for the power flows at higher frequencies are around 30% smaller than for excitations in x-direction.

The wing structure is even more stiff in y-direction than it is in x-direction. Similar to the comparison between excitations in z- and x-direction this is the reason why the power flows for excitations in y-direction further decrease. Imagine a one-sided clamped beam with a force exciting it along the beam axis from the free end. This beam will have a certain stiffness for its respective length. When the same force excites the beam but not from the free end but at the half length of the beam the stiffness of this beam part will be much higher. The same excitation force will result in less power input into the beam.

Nevertheless, power flows increase again with frequency but there is no clear trend forming that shows higher power flows entering the CWB for excitations closer to the fuselage. A possible reason why no clear trend is forming might be that for the excitations in y-direction not only bending waves are induced (due to the eccentricity of the excitation in respect to the CWB symmetry) but also a ratio of longitudinal waves is introduced into the structure. This might result in more complex resonances than for the previous two excitations.

4. CONCLUSION & OUTLOOK

This paper investigates the transport of vibratory power due to dynamic loads generated from operation of jet engines installed on an aircraft wing. In particular, the amount of vibratory power injected into the center wing box and thus injected into the aircraft fuselage will be studied for different engine installation positions. The excitation by dynamic loads introduced into wing structure will lead to a transport of vibratory power throughout the structure.

The results of this study show that for higher frequencies the power flows entering the center wing box will increase for decreasing distances between excitations and the fuselage structure. Vibrations introduced by the jet engine in vertical direction (wing lift direction) result in power flows three times larger than for excitations in other directions. Additionally, the power flows resulting from vibrations introduced in x-direction (flight direction or engine thrust direction) is 50% higher in comparison to the third excitation investigated which introduces vibrations in y-direction (wing span direction) but only for higher frequency bands. The different magnitudes of power flow in the different directions can be explained with the different elastic stiffnesses of the wing in the different directions. The stiffness for bending in vertical direction is much less than for bending in wing in-plane direction. In addition, the excitation in y-direction (lateral direction) will additionally cause extension/compression deformation instead of pure bending, for which the wing stiffness is again higher that for in-plane bending.

In general, the model results in physically reasonable results. However, for future investigations the model needs to be improved in some aspects. At first, the model used here contains realistic stiffened structural parts for pylon attachments. This has only been used for the initial engine position “2”, see Figure 3. When changing the excitation position to “1” or “3”, the structural interface to the pylon did not change but remained at position “2”. In future studies the FE model needs to be adapted to contain realistic stiffening at all excitation positions. Furthermore, realistic vibration loads consisting of load combinations in the three excitation directions need to be used. This will lead to load cases and related detailed results closer to real operation conditions instead of the generic excitations used for this initial study. Most importantly will be the updating of the FE model with experimental data. Not only for the main wing structure itself but also for the boundary condition at the structural interface to the other parts of the aircraft, which are not modelled here but which may receive vibratory energy from engine operation. Furthermore, a comparison between the resulting power flows entering the center wing box and the actual power input by the excitations is inevitable. Subsequently, it will be possible to draw more detailed insights from this model and provide better comparisons for the contributions of different excitation directions to the power flows entering the center wing box.

5. ACKNOWLEDGEMENTS

This project has received funding from the Clean Sky 2 Joint Undertaking under the European Union’s Horizon 2020 research and innovation programme under grant agreement N° CS2-LPA-GAM-2014-2015-01.

6. REFERENCES

1. Airbus A320 Scale Model and wing cut out. https://www.turbosquid.com/3d-models/airbus-a320-scale-model-3d-model-1766910
2. Norambuena, Marco und Winter, Rene (2019) An adaptive structural excitation system as a tool for structure-borne noise research. In: Proceedings of the 23rd International Congress on Acoustics: Integrating 4th EAA Euroregio 2019.
3. Hambric, S. A. (1990). "Power flow and mechanical intensity calculations in structural finite element analysis." Journal of Vibration and Acoustics 112(4): 542-549.
4. Klimmek, T. und Schulze, M. und Abu-Zurayk, M. und Ilic, C. und Merle, A. (2019). “cpacsMONA – An independent and in high fidelity based MDO tasks integrated process for the structural and aeroelastic design for aircraft configurations.” Proceedings of the IFASD 2019.
5. Gavric, L., Pavic, G. (1993). "A finite-element method for computation of structural intensity by the normal-mode approach." Journal of Sound and Vibration 164(1): 29-43.
6. Niu, M. C.-Y. (1988). Airframe Structural Design. Burbank, California, USA, Conmilit Press Ltd.
7. Biedermann, J., et al. (2017). Classification of the mid-frequency range based on spatial Foruer decomposition of operational deflection shapes. International Congress on Sound and Vibration. London.
8. Lyon, H. and R. G. DeJong (1994). Theory and application of statistical energy analysis.
9. Tanner, G. (2008). "Dynamical energy analysis - Determining wave energy distributions in vibroacoustical structures in the high-frequency regime." *Journal of Sound and Vibration* **320**: 1023–1038.